Supramolecular Chemistry

DOI: 10.1002/anie.201407144

Self-Assembly of a Giant Molecular Solomon Link from 30 Subcomponents**

*Clément Schouwey, Julian J. Holstein, Rosario Scopelliti, Konstantin O. Zhurov, Konstantin O. Nagornov, Yury O. Tsybin, Oliver S. Smart, Gérard Bricogne, and Kay Severin**

Abstract: *The synthesis of topologically complex structures, such as links and knots, is one of the current challenges in supramolecular chemistry. The so-called Solomon link consists of two doubly interlocked rings. Despite being a rather simple link from a topological point of view, only few molecular versions of this link have been described so far. Here, we report the quantitative synthesis of a giant molecular Solomon link from 30 subcomponents. The highly charged structure is formed by assembly of 12 cis-blocked Pt^{2+} complexes, six Cu^{+} ions, and 12 rigid N-donor ligands. Each of the two interlocked rings is composed of six repeating Pt(ligand) units, while the six Cu^{+} ions connect the two rings. With a molecular weight of nearly 12 kDa and a diameter of 44.2 Å, this complex is the largest non-DNA-based Solomon link described so far. Furthermore, it represents a molecular version of a "stick link".*

Knots are ubiquitous in our daily life. However, the mathematical definition of a knot differs from the everyday concept, as it applies to the entanglement of a closed loop instead of loose strings. Two or more interlocked knots are termed (nontrivial) links. The number of knots and links is theoretically infinite[1] and more than six billion prime knots (i.e. knots that cannot be obtained by combining other knots) have already been tabulated.[2] The chemical realm, in comparison, comprises to date only a few of the simplest structures. Excluding DNA-based structures, chemists were able to synthesize three different types of knots: trefoil knots,[3,4] composite knots,[5] and a pentafoil knot.[6,7] The following types of links have also been reported: a range of [*n*]catenanes,[7] Borromean rings,[8] and Solomon links.[3,9] Solomon links consist of two trivial unknots (i.e. rings), which cross each other four times, each ring crossing alternatively below and above the other. As of today, only a few examples of molecular Solomon links have been described.[3,9]

The first syntheses of Solomon links, reported by the group of Sauvage, relied on the assembly of cyclic helicates by metal templation (Cu^{+} or Li^{+}), followed by covalent capture through cyclisation reactions.[9f,h] Subsequently, the groups of Sauvage and Fujita reported the quantitative formation of a Solomon link by self-assembly. The two macrocycles of the link were obtained by reaction of *cis*-blocked Pd^{2+} complexes and N-donor ligands, and entanglement was induced by Cu^{+} ions.[9g] A schematic representation of the resulting link is shown in Figure 1 a. Following these pioneering studies, some other groups have succeeded in synthesizing Solomon links using self-assembly processes.[9a–e] Several of these links feature macrocycles with dynamic covalent imine bonds, which are linked by metal ions (Figure 1 b).[3,9b,d] It is worth noting that the reactions by self-assembly are all based on two different reversible interactions, which are largely orthogonal to each other.[10] One of the interactions is used to form the rings, whereas the second one controls the topology of the entanglement.

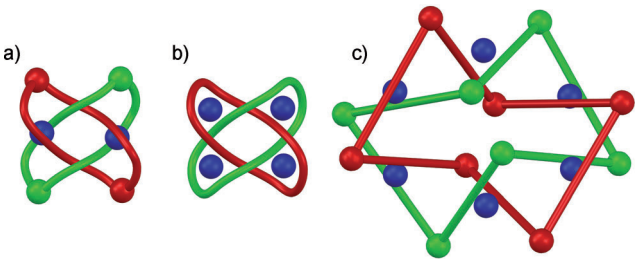

Figure 1. Schematic representation of Solomon links obtained by self-assembly. a) A link based on two dinuclear metallamacrocycles and two bridging metal ions.[9g] b) A link based on two dynamic covalent macrocycles and four bridging metal ions.[9d] c) The link described in the present work based on two hexanuclear metallamacrocycles and six bridging metal ions. The graphics for (b) and (c) are based on crystallographic data. Therefore, they are on the same scale.

Below, we describe the synthesis and characterization of a molecular Solomon link, which is significantly larger and more complex than the synthetic links described above. The basis of our work was a well-known principle in metallasupramolecular chemistry: flexible bridging ligands tend to favor small aggregates.[11] We therefore wondered what would

[*] Dr. C. Schouwey, Dr. R. Scopelliti, K. O. Zhurov, Dr. K. O. Nagornov, Prof. Y. O. Tsybin, Prof. K. Severin
Institut des Sciences et Ingénierie Chimiques
Ecole Polytechnique Fédérale de Lausanne (EPFL)
1015 Lausanne (Switzerland)
E-mail: kay.severin@epfl.ch
Dr. J. J. Holstein,[+] Dr. O. S. Smart, Dr. G. Bricogne
Global Phasing Ltd., Sheraton House
Castle Park, Cambridge CB3 0AX (UK)
[+] Current address: GZG, Abteilung Kristallographie
Georg-August-Universität Göttingen
Goldschmidtstr. 1, 37077 Göttingen (Germany)

[**] This work was supported by funding from the Swiss National Science Foundation, a Marie Curie fellowship for J.J.H. (ITN-2010-264645), and by the EPFL. We thank Dr. Pascal Miéville for his help with DOSY experiments, and Prof. Dr. Anthony L. Spek for providing updated CHECKCIF routines to handle structures of the Solomon link's size.

Supporting information for this article is available on the WWW under http://dx.doi.org/10.1002/anie.201407144.

happen if we replace the bent and flexible ligand that gave rise to a hexanuclear $M_2M'_4L_4$ Solomon link (Figure 1a)[9g] with a ligand possessing similar binding sites, but which is linear and rigid. We found that a considerably larger $M_6M'_{12}L_{12}$ complex was formed (Figure 1c), whereas the Solomon link topology was maintained. Details of these findings are reported below.

The formation of square-shaped molecular structures by reaction of linear ditopic N-donor ligands with *cis*-blocked Pt^{2+} and Pd^{2+} complexes is well understood.[11] The square motif is tolerant to the functionalization of the N-donor ligand, for example with dendrons,[12] pseudorotaxanes,[13] and salen-type binding sites.[14] However, depending on the rigidity of the ligand and the bulkiness of the *cis*-blocking ligands, smaller triangular structures can also be formed, typically in equilibrium with the squares.[11,15]

Cu^+ cations form tetrahedral complexes with 2,2′-bipyridine (bipy) or with the related 1,10-phenanthroline ligand (phen). The $[Cu(phen)_2]^+$ motif has been used extensively for the metal-directed synthesis of complex molecular architectures.[7] For example, it was used in combination with Pd^{2+} for the assembly of a Solomon link,[9g] or in combination with Zn,[16] Ru,[17] and Rh[18] complexes for the synthesis of [2]catenanes. In contrast, the $[Cu(bipy)_2]^+$ motif has rarely been employed in this context.[19]

We were interested in combining these two binding patterns in a single ligand and therefore synthesized ligand **1**, which possesses both a bipy core for Cu^+ coordination and terminal pyridine groups for Pt^{2+} coordination. We used bipy instead of phen because the synthesis of the ligand was more convenient, and because we did not expect any significant difference in the coordination behavior. The synthesis of this ligand was indeed straightforward and proceeded in three steps from the commercially available 3-bromo-6-iodo-2-methylpyridine, with an overall yield of 40% (see the Supporting Information, SI). We decided to incorporate two methyl groups in **1** to increase the solubility of the ligand and the selectivity of the central binding site for Cu^+ over (dppp)Pt^{2+} (dppp = 1,3-bis(diphenylphosphino)propane). We reasoned that the methyl groups would cause an unfavorable steric interaction with the dppp ligand and favor the coordination of the competitor Cu^+ at the central binding site.

The regioselectivity of the reaction of ligand **1** with Cu^+ and (dppp)Pt^{2+} was investigated by NMR spectroscopic analysis of solutions containing **1** and 0.5 equivalents of $Cu(MeCN)_4(BF_4)$ or one equivalent of (dppp)$Pt(OTf)_2$ (CD_2Cl_2/CD_3OD 1:1, v/v). The NMR spectra of the mixture containing $Cu(MeCN)_4(BF_4)$ revealed only one set of signals (Figures S13 and S14), consistent with the selective formation of complex **2** (Scheme 1). The coordination of Cu^+ induced a pronounced shift of the ^1H NMR signals of protons A and B ($\Delta\delta = 0.17$ and 0.33 ppm), whereas the signals of the protons C and D were hardly affected ($\Delta\delta = 0.02$ and 0.03 ppm), further suggesting that Cu^+ is bound to the bipy core.

^1H, ^{13}C and ^{31}P NMR analysis of a 1:1 solution of **1** and (dppp)$Pt(OTf)_2$ revealed the formation of two different products (Figures S10–S12), which were found to be of different size as determined by diffusion ordered spectroscopy (DOSY) analysis (Figure S17). This time, significant differences in chemical shifts were observed for the signals of protons C and D ($\Delta\delta = 0.34$ and 0.21 ppm for the most abundant species, 0.22 and 0.26 ppm for the other one), suggesting that, in both cases, Pt^{2+} is bound to the terminal pyridine groups. We hypothesized that the two products were the square **3** and the triangle **4** (Scheme 1). To confirm that the two products were indeed **3** and **4**, we determined the distribution of the two products at a total Pt^{2+} concentration of 12.30 mM, 6.15 mM, and 2.05 mM. In line with our assumption, the relative abundance of **4** with respect to **3** increased upon dilution from [**4**]:[**3**] = 0.5 to [**4**]:[**3**] = 0.8. By using the integrals of the signal of protons D and the equation $K_{3,4} = [\mathbf{4}]^4/[\mathbf{3}]^3$, very similar $K_{3,4}$ values of 1.3×10^{-4} M, 1.4×10^{-4} M, and 1.3×10^{-4} M were obtained for the three concentrations, coherent with a triangle-square equilibrium.

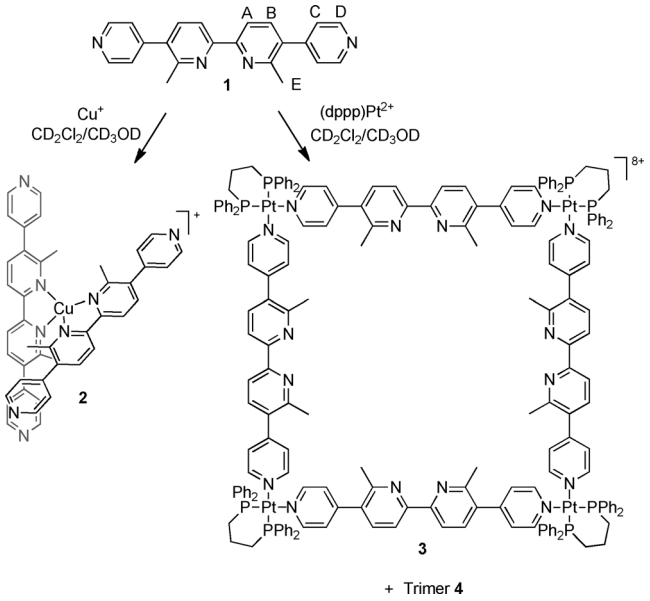

Scheme 1. Reactions of ligand **1** with $Cu(MeCN)_4BF_4$ or (dppp)$Pt(OTf)_2$.

The presence of both complexes **3** and **4** was verified using a high resolution 10 T FT-ICR mass spectrometer with a chip-based nanoESI source (see SI for details).[20] A 20 μM solution of **3** and **4** was used, isotopic clusters corresponding to $[(\mathbf{3})(OTf)_6]^{2+}$ and $[(\mathbf{4})(OTf)_4]^{2+}$ were detected, and the isotopic distribution of both clusters was compared with theoretical distributions (Figures S18 and S19).[21] Ions of both clusters were separately isolated in the gas phase and irradiated with a CO_2 laser beam until fragmentation was achieved: the resultant fragment ions corresponded to [(**1**)-(dppp)$Pt(OTf)]^+$ and other related species. Mass accuracies for isolated precursor ions and generated fragment ions were better than 5 ppm in all cases.

The presence of square **3** was additionally confirmed by single-crystal X-ray diffraction analysis. Upon diffusion of Et_2O in a mixture of $\mathbf{3}(OTf)_8$ and $\mathbf{4}(OTf)_6$ in DCM/MeOH 1:1, v/v, colorless crystals were obtained. Crystallographic analyses revealed the expected square structure of **3** (Figure 2).[22] The N-Pt-N angles have values comprised between 83–85°, similar to what was reported for other square structures based

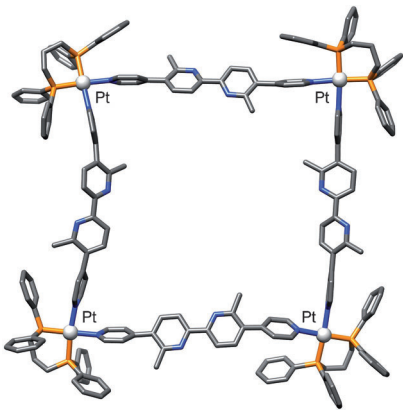

Figure 2. Structure of square **3** in the solid state. Solvent molecules, hydrogen atoms, and counteranions are omitted for clarity. Color coding: gray C, blue N, orange P, white Pt.

on bisphosphine Pt corners.[15c,23] The average Pt···Pt distance between two adjacent centers is 19.5 Å and the maximal Pt···Pt distance between opposed corners of the macrocycle is 26.5 Å. Because no crystals of **4**$(OTf)_6$ were obtained, we assume that square **3**$(OTf)_8$ crystalizes selectively out of the mixture. Overall, the control experiments with either Cu$(MeCN)_4BF_4$ or (dppp)Pt$(OTf)_2$ demonstrate that the complexation of **1** to Cu^+ and (dppp)Pt^{2+} is highly selective.

Next, we investigated the reaction of **1** with both metal salts at the same time using a stoichiometry of **1**:Cu:Pt = 2:1:2. At first, the ^{1}H NMR spectrum of the mixture showed multiple broad peaks suggesting the presence of a complex mixture of species. Over the course of two days, it transformed into a well-resolved but complex spectrum (Figure S15). For ligand **1**, six sets of signals with the same intensity were observed (Figure S6). A similar sixfold splitting was observed in the ^{13}C NMR spectrum (Figures S8 and S9). The ^{31}P spectrum was less informative due to the small chemical shift difference between the signals leading to very poor peak separation (Figure S7). DOSY analysis confirmed that all signals in the ^{1}H NMR spectrum belong to a single species with a diffusion coefficient smaller than the one of **3** (Figure S16).

Taken together, the NMR data suggested that a defined product of low symmetry had formed in nearly quantitative yield. Complex **5**$(OTf)_{24}(BF_4)_6$ could be isolated as a red microcrystalline powder in 81% yield by addition of Et_2O. NMR analyses of the isolated product revealed spectra identical to the ones obtained for the reaction mixture after two days.

The composition of the cation **5** was analyzed by mass spectrometry using the same instrumental set up as for complexes **3** and **4**: several clusters corresponding to a $[Pt_{12}(dppp)_{12}(\mathbf{1})_{12}Cu_6]^{30+}$ core were detected, with varying number of triflate counterions, typically between 20–22, attached (Figure S20). Additional peaks corresponding to the fragmentation of the parent structure were also observed. The theoretical distribution of $[(\mathbf{5})(OTf)_{24}]^{6+}$ (Figure S21) matches well with the experimental distribution and the fragmentation of the isolated species results mainly in $[Cu(\mathbf{1})_2]^+$ and $[(\mathbf{1})(dppp)Pt(OTf)]^+$ fragments, confirming the assignment (Figure S22).

The structure of complex **5**$(OTf)_{24}(BF_4)_6$ was elucidated by single-crystal X-ray analysis (Figure 3).[22] The refinement of the crystallographic data of this huge complex represented a special challenge. Its unit cell volume of 204881(3) Å^3 is in the range found for small proteins. Disordered solvent/anion areas occupy 56% of the unit cell, which results in a limited scattering power of the crystals (only) up to 1.2 Å resolution. Standard small molecule approaches are insufficient to tackle supramolecular structures with these characteristics, and only a series of carefully adapted macromolecular refinement techniques enabled us to overcome this challenge and

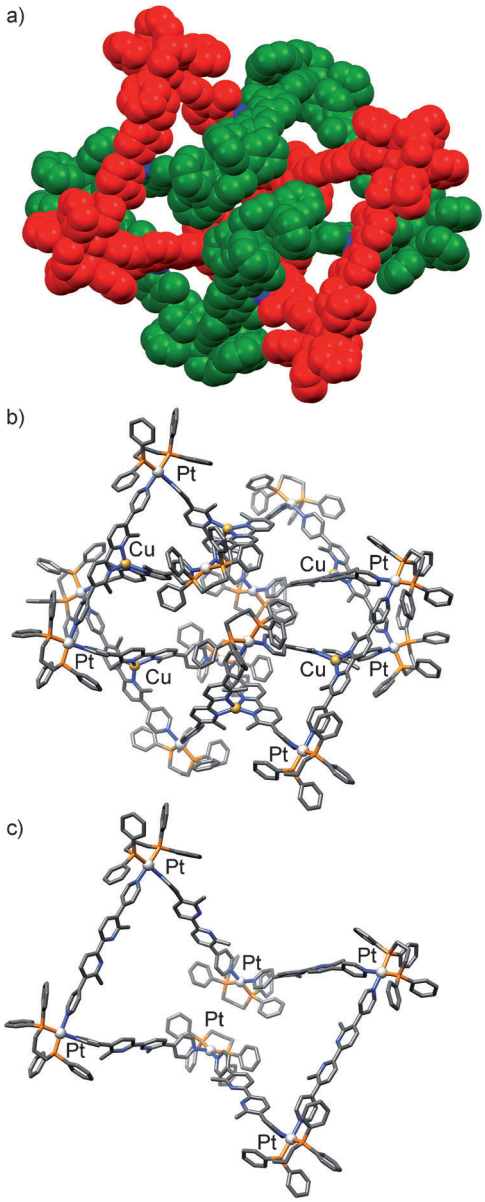

Figure 3. Structure of the Solomon link in the solid state. a) Space filling representation; b) ball and stick representation; c) ball and stick representation of a hexanuclear $[Pt_6(dppp)_6(\mathbf{1})_6]^{12+}$ macrocycle. Solvent molecules, hydrogen atoms, and counteranions are omitted for clarity. Color coding for (b) and (c): gray C, blue N, orange P, white Pt.

complete the structural model. As in other cases of huge and complicated supramolecular structures with high solvent content,[24,25] the application of geometric restraint dictionaries generated with the Grade Web Server[26] and rigid bond restraints[27] were key for successfully building a complete molecular model. Local structural similarity restraints (LSSR) exploiting noncrystallographic symmetry (NCS)[28] were additionally applied here. All three types of restraints are specifically designed for macromolecular structure determinations,[26,28] and only their combined use enabled us to determine the composition and the connectivity of **5** with reasonably good precision. The asymmetric unit contains two full Solomon links. Due to crystallization in the centrosymmetric space group $P2_1/n$ one finds a racemic mixture of both enantiomers of the chiral link in the unit cell,[29] and a total of 1447 independent (nonhydrogen) atoms.

Complex **5** has the composition $[Pt_{12}(dppp)_{12}(\mathbf{1})_{12}Cu_6]^{30+}$. One can observe two hexanuclear $Pt_6(dppp)_6(\mathbf{1})_6$ macrocycles, which are doubly interlocked to form a Solomon link (Figure 3). The individual Pt-macrocycles form a butterfly-like structure. To the best of our knowledge, the formation of hexanuclear macrocycles from *cis*-blocked Pt^{2+} complexes and linear N-donor ligands is unprecedented. The average N-Pt-N angles are comprised between 82–88° (mean 85°), similar to the one observed for square **3**. The average Pt···Pt distance between two adjacent centers is 19.5 Å, and the maximal Pt···Pt distance between opposed corners of the macrocycles is 34.0 Å. The two Pt-macrocycles are connected by six Cu^+ cations, which are coordinated to the bipy part of the ligand (Figure 3).

The solid state structure of **5** is coherent with all the spectroscopic data obtained from solution-based studies. The molecular weight of the species detected by mass spectrometry analysis is in line with the composition of complex **5**. The low apparent symmetry detected by NMR spectroscopy is a reflection of the low symmetry of the linked macrocycles. Indeed, **5** possesses three rotational C_2 axes. As a consequence, there are three different sets of equivalent ligands **1** in complex **5**. As each ligand is linked to two nonequivalent Pt centers, the internal symmetry of the ligand **1** is broken and the two halves are no longer magnetically equivalent, leading to 3×2 different signals. Similarly, the two P atoms on each of the three different Pt centers are magnetically different, in line with the complexity of the ^{31}P NMR spectrum observed for **5**. The fact that **5** was obtained as the sole product after equilibration suggests that the complex is formed under thermodynamic control.[30] Most likely, it is not possible to form smaller aggregates containing $[Pt(dppp)(\mathbf{1})]_n$ rings and $[Cu(\mathbf{1})_2]$ complexes without energetic penalization.

To conclude: A molecular Solomon link was obtained by self-assembly of 30 components. The two interlocked rings of the link consist of $Pt_6(dppp)_6(\mathbf{1})_6$ macrocycles with an unusual butterfly-like structure. The two Pt-macrocycles are connected by six Cu^+ ions. With a molecular weight of nearly 12 kDa and a diameter of 44.2 Å (max. C···C distance), complex **5** is the largest non-DNA-based Solomon link described so far.[31] Conceptually, the synthesis of **5** is similar to that of the first self-assembled Solomon link reported in 1999.[9g] In both cases, the links were formed from square planar metal complexes, Cu^+ ions, and tritopic N-donor ligands with terminal pyridyl groups and internal N–N chelate binding sites. The key difference of our new approach is the utilization of a linear and rigid ligand.[32] For the synthesis of metallomacrocyclic structures, it is well established that restricting the conformational flexibility of the building blocks can result in larger assemblies. The successful formation of **5** demonstrates that this simple concept can also be applied to topologically complex molecules such as Solomon links.

Knots and links can be represented in different ways, and, as discussed in a recent review article,[7b] the way a knot is represented will affect the synthetic strategy to obtain it. Interestingly, all figures depicting knots in the aforementioned review use curved traits, in line with the ubiquitous use of nonlinear ligands for the synthesis of interlocked molecules. Our results show that linear linkers are interesting alternatives.

Some inspiration for future work can be found in knot theory, as mathematicians have already coined the term "stick knots" for those knots based on linear components.[33] 3D models of minimal stick knots and links are available on the web.[34,35] Encouragingly for chemists, equilateral stick knots, which would require only one type of bridging ligand, are not significantly more complex than regular stick knots.[36]

Received: July 12, 2014
Published online: August 28, 2014

Keywords: copper · molecular link · platinum · self-assembly · topology

[1] J. Hoste in *Handbook of Knot Theory* (Eds.: W. Menasco, M. Thistlethwaite), Elsevier Science Amsterdam, **2005**, pp. 209–232.

[2] a) S. Rankin, O. Flint, J. Schermann, *J. Knot Theory Ramifications* **2004**, *13*, 57–100; b) S. Rankin, O. Flint, J. Schermann, *J. Knot Theory Ramifications* **2004**, *13*, 101–149.

[3] T. Prakasam, M. Lusi, M. Elhabiri, C. Platas-Iglesias, J.-C. Olsen, Z. Asfari, S. Cianférani-Sanglier, F. Debaene, L. J. Charbonnière, A. Trabosi, *Angew. Chem. Int. Ed.* **2013**, *52*, 9956–9960; *Angew. Chem.* **2013**, *125*, 10140–10144.

[4] a) N. Ponnuswamy, F. B. L. Cougnon, J. M. Clough, G. D. Pantoş, J. K. M. Sanders, *Science* **2012**, *338*, 783–785; b) P. E. Barran, H. L. Cole, S. M. Godup, D. A. Leigh, P. R. McGonial, M. D. Symes, J. Wu, M. Zengerle, *Angew. Chem. Int. Ed.* **2011**, *50*, 12280–12284; *Angew. Chem.* **2011**, *123*, 12488–12492; c) J. Guo, P. C. Mayers, G. A. Breault, C. A. Hunter, *Nat. Chem.* **2010**, *2*, 218–222; d) M. Feigel, R. Ladberg, S. Engels, R. Herbst-Irmer, R. Fröhlich, *Angew. Chem. Int. Ed.* **2006**, *45*, 5698–5702; *Angew. Chem.* **2006**, *118*, 5827–5831; e) L.-E. Perret-Aebi, A. von Zelewsky, C. Dietrich-Buchecker, J.-P. Sauvage, *Angew. Chem. Int. Ed.* **2004**, *43*, 4482–4485; *Angew. Chem.* **2004**, *116*, 4582–4585; f) O. Safarowsky, M. Nieger, R. Fröhlich, F. Vögtle, *Angew. Chem. Int. Ed.* **2000**, *39*, 1616–1618; *Angew. Chem.* **2000**, *112*, 1699–1701; g) G. Rapenne, C. Dietrich-Buchecker, J.-P. Sauvage, *J. Am. Chem. Soc.* **1999**, *121*, 994–1001; h) C. Dietrich-Buchecker, G. Rapenne, *Chem. Commun.* **1997**, 2053–2054; i) P. R. Ashton, O. A. Matthews, S. Menzer, F. M. Raymo, N. Spencer, J. F. Stoddart, D. J. Williams, *Liebigs Ann.* **1997**, 2485–2494; j) C. Dietrich-Buchecker, J.-P. Sauvage, A. D. Cian, J. Fischer, *J. Chem. Soc. Chem. Commun.* **1994**, 2231–2232.

[5] R. F. Carina, C. Dietrich-Buchecker, J.-P. Sauvage, *J. Am. Chem. Soc.* **1996**, *118*, 9110 – 9116.

[6] a) J.-F. Ayme, J. E. Beves, D. A. Leigh, R. T. McBurney, K. Rissanen, D. Schultz, *J. Am. Chem. Soc.* **2012**, *134*, 9488 – 9497; b) J.-F. Ayme, J. E. Beves, D. A. Leigh, R. T. McBurney, K. Rissanen, D. Schultz, *Nat. Chem.* **2012**, *4*, 15 – 20.

[7] For reviews see: a) J.-F. Ayme, J. E. Beves, C. J. Campbell, D. A. Leigh, *Chem. Soc. Rev.* **2013**, *42*, 1700 – 1712; b) J.-C. Chambron, J.-P. Sauvage, *New J. Chem.* **2013**, *37*, 49 – 57; c) R. S. Forgan, J.-P. Sauvage, J. F. Stoddart, *Chem. Rev.* **2011**, *111*, 5434 – 5464; d) J. E. Beves, B. A. Blight, C. J. Campbell, D. A. Leigh, R. T. McBurney, *Angew. Chem. Int. Ed.* **2011**, *50*, 9260 – 9327; *Angew. Chem.* **2011**, *123*, 9428 – 9499.

[8] a) S.-L. Huang, Y.-J. Lin, T. S. A. Hor, G.-J. Jin, *J. Am. Chem. Soc.* **2013**, *135*, 8125 – 8128; b) C. D. Pentecost, A. J. Peters, K. S. Chichak, G. W. V. Cave, S. J. Cantrill, J. F. Stoddart, *Angew. Chem. Int. Ed.* **2006**, *45*, 4099 – 4104; *Angew. Chem.* **2006**, *118*, 4205 – 4210; c) K. S. Chichak, A. J. Peters, S. J. Cantrill, J. F. Stoddart, *J. Org. Chem.* **2005**, *70*, 7956 – 7962; d) K. S. Chichak, S. J. Cantrill, A. R. Pease, S.-H. Chiu, G. W. V. Cave, J. L. Atwood, J. F. Stoddart, *Science* **2004**, *304*, 1308 – 1312.

[9] a) N. Ponnuswamy, F. B. L. Cougnon, G. D. Pantos, J. K. M. Sanders, *J. Am. Chem. Soc.* **2014**, *136*, 8243 – 8261; b) J. E. Beves, C. J. Campbell, D. A. Leigh, R. G. Pritchard, *Angew. Chem. Int. Ed.* **2013**, *52*, 6464 – 6467; *Angew. Chem.* **2013**, *125*, 6592 – 6595; c) C. Peinador, V. Blanco, J. M. Quintela, *J. Am. Chem. Soc.* **2009**, *131*, 920 – 921; d) C. D. Pentecost, K. S. Chichak, A. J. Peters, G. W. V. Cave, S. J. Cantrill, J. F. Stoddart, *Angew. Chem. Int. Ed.* **2007**, *46*, 218 – 222; *Angew. Chem.* **2007**, *119*, 222 – 226; e) C. P. McArdle, J. J. Vittal, R. J. Puddephatt, *Angew. Chem. Int. Ed.* **2000**, *39*, 3819 – 3822; *Angew. Chem.* **2000**, *112*, 3977 – 3980; f) C. Dietrich-Buchecker, J.-P. Sauvage, *Chem. Commun.* **1999**, 615 – 616; g) F. Ibukuro, M. Fujita, K. Yamaguchi, J.-P. Sauvage, *J. Am. Chem. Soc.* **1999**, *121*, 11014 – 11015; h) J. F. Nierengarten, C. Dietrich-Buchecker, J.-P. Sauvage, *J. Am. Chem. Soc.* **1994**, *116*, 375 – 376.

[10] M. N. Saha, S. De, S. Pramanik, M. Schmittel, *Chem. Soc. Rev.* **2013**, *42*, 6860 – 6909.

[11] a) R. Chakrabarty, P. S. Mukherjee, P. J. Stang, *Chem. Rev.* **2011**, *111*, 6810 – 6918; b) F. Würthner, C.-C. You, C. R. Saha-Möller, *Chem. Soc. Rev.* **2004**, *33*, 133 – 146.

[12] H. T. Baytekin, M. Sahre, A. Rang, M. Engeser, A. Schulz, C. A. Schalley, *Small* **2008**, *4*, 1823 – 1834.

[13] K.-M. Park, S.-Y. Kim, J. H, D. Whang, S. Sakamoto, K. Yamaguchi, K. Kim, *J. Am. Chem. Soc.* **2002**, *124*, 2140 – 2147.

[14] S.-S. Sun, C. L. Stern, S. T. Nguyen, J. T. Hupp, *J. Am. Chem. Soc.* **2004**, *126*, 6314 – 6326.

[15] a) T. Weilandt, R. W. Troff, H. Saxell, K. Rissanen, C. A. Schalley, *Inorg. Chem.* **2008**, *47*, 7588 – 7598; b) M. Ferrer, M. Mounir, O. Rossell, E. Ruiz, M. A. Maestro, *Inorg. Chem.* **2003**, *42*, 5890 – 5899; c) M. Schweiger, S. R. Seidel, A. M. Arif, P. J. Stang, *Inorg. Chem.* **2002**, *41*, 2556 – 2559; d) A. Sautter, D. G. Schmid, G. Jung, F. Würthner, *J. Am. Chem. Soc.* **2001**, *123*, 5424 – 5430; e) M. Fujita, O. Sasaki, T. Mitsahashi, T. Fujita, J. Yazaki, K. Yamaguchi, *Chem. Commun.* **1996**, 1535 – 1536.

[16] M. Beyler, V. Heitz, J.-P. Sauvage, *Chem. Commun.* **2008**, 5396 – 5398.

[17] B. X. Colasson, J.-P. Sauvage, *Inorg. Chem.* **2004**, *43*, 1895 – 1901.

[18] M. Beyler, V. Heitz, J.-P. Sauvage, *New J. Chem.* **2010**, *34*, 1825 – 1829.

[19] J. R. Price, J. K. Clegg, R. R. Fenton, L. F. Lindoy, J. C. McMurtrie, G. V. Meehan, A. Parkin, D. Perkins, P. Turner, *Aust. J. Chem.* **2009**, *62*, 1014 – 1019.

[20] H. Ben Hamidane, A. Vorobyev, Y. O. Tsybin, *Eur. J. Mass Spectrom.* **2011**, *17*, 321 – 331.

[21] L. Patiny, A. Borel, *J. Chem. Inf. Model.* **2013**, *53*, 1223 – 1228.

[22] CCDC 1001443 (**3**) and 1001444 (**5**) contain the supplementary crystallographic data for this paper. These data can be obtained free of charge from The Cambridge Crystallographic Data Centre via www.ccdc.cam.ac.uk/data_request/cif.

[23] P. J. Stang, D. H. Cao, S. Saito, A. M. Arif, *J. Am. Chem. Soc.* **1995**, *117*, 6273 – 6283.

[24] T. K. Ronson, C. Giri, N. K. Beyeh, A. Minkkinen, F. Topić, J. J. Holstein, K. Rissanen, J. Nitschke, *Chem. Eur. J.* **2013**, *19*, 3374 – 3382.

[25] M. Pascu, M. Marmier, C. Schouwey, R. Scopelliti, J. J. Holstein, G. Bricogne, K. Severin, *Chem. Eur. J.* **2014**, *20*, 5592 – 5600.

[26] http://grade.globalphasing.org.

[27] A. Thorn, B. Dittrich, G. M. Sheldrick, *Acta Crystallogr. Sect. A* **2012**, *68*, 448 – 451.

[28] O. S. Smart, T. O. Womack, C. Flensburg, P. Keller, W. Paciorek, A. Sharff, C. Vonrhein, G. Bricogne, *Acta Crystallogr. Sect. D* **2012**, *68*, 368 – 380.

[29] C. Liang, K. Mislow, *J. Math. Chem.* **1995**, *18*, 1 – 24.

[30] Since complex **5** is formed under thermodynamic control, it appears unlikely that Cu^{+} can be removed without structural rearrangement.

[31] For DNA-based knots and links, see: a) T. Ciengshin, R. Sha, N. C. Seeman, *Angew. Chem. Int. Ed.* **2011**, *50*, 4419 – 4422; *Angew. Chem.* **2011**, *123*, 4511 – 4514; b) N. C. Seeman, *Acc. Chem. Res.* **1997**, *30*, 357 – 363.

[32] For bent ligands containing a central *N*,*N*′-binding site and terminal pyridyl groups see Ref. [9g] and: a) M. Schmittel, B. He, J. Fan, J. W. Bats, M. Engeser, M. Schlosser, H.-J. Deiseroth, *Inorg. Chem.* **2009**, *48*, 8192 – 8200; b) O. V. Dolomanov, A. J. Blake, N. R. Champness, M. Schröder, C. Wilson, *Chem. Commun.* **2003**, 682 – 683.

[33] E. A. Elrifai, *Chaos Solitons Fractals* **2006**, *27*, 233 – 236.

[34] http://www.colab.sfu.ca/KnotPlot/sticknumbers/index.html.

[35] http://www.colab.sfu.ca/KnotPlot/sticknumbers/links/.

[36] E. J. Rawdon, R. G. Scharein, *Contemp. Math.* **2002**, *304*, 55 – 75.

